ROSETTA NAVIGATION FROM REACTIVATION UNTIL ARRIVAL AT COMET 67P/CHURYUMOV-GERASIMENKO

Trevor Morley(1), Frank Budnik(2), Bernard Godard(1), Pablo Muñoz(3) and Vishnu Janarthanan(4)

(1)*Telespazio VEGA Deutschland GmbH, located at ESOC*
(2)*ESA/ESOC*
(3)*GMV, located at ESOC*
(4)*Terma GmbH, located at ESOC*
Robert-Bosch-Strasse 5, D-64293 Darmstadt, Germany +49 6151 900
<firstname>.<lastname>@esa.int

Abstract: *After 31 months in hibernation and no contact with the ground, Rosetta autonomously reactivated itself on 20th January 2014. There was no problem for accurate pointing of the ground antennas to receive the spacecraft signal. Thereafter, frequent orbit determinations were made using two-way Doppler and range data acquired by both ESA and NASA deep space stations. Initially, the determination of the comet's orbit had to rely on only ground-based astrometric data. On 20th March, the comet was detected by the science narrow angle camera. The ensuing optical navigation using the data from the reduction of camera images much improved the knowledge of the comet's state relative to Rosetta. From 8th May onwards, the same data were additionally obtained with the navigation cameras. On 7th May the first of 10 trajectory control manoeuvres was executed to reduce in steps the spacecraft's relative velocity. During this period, the conventional radiometric measurements were augmented with delta differential one-way range data. A problem with the degraded quality of these data was solved and the cause for seemingly slightly anomalous Doppler data after the large manoeuvres was explained. All the manoeuvres were executed at the expected times and, with one minor exception, showed excellent performance. Rosetta arrived safely on 6th August 2014 and was inserted into its initial hyperbolic orbit around the comet.*

Keywords: *Rosetta, comet 67P/Churyumov-Gerasimenko, deep space navigation.*

1. Introduction

1.1 Rosetta Mission

Rosetta was injected directly into an Earth escape trajectory on 2nd March 2004. To rendezvous with comet 67P/Churyumov-Gerasimenko (67P/C-G), the spacecraft made three Earth swing-bys [1], each of which increased the orbital energy, and one Mars swing-by [2] that decreased the energy but optimised the phasing for the third Earth swing-by that gave the largest energy boost. During its solar system cruise, Rosetta made close fly-bys of asteroids (2867) Šteins [3] and (21) Lutetia [4].

As planned before launch, on 8th June 2011, when it was 4.49 au from the Sun, Rosetta was put into hibernation. At the higher heliocentric distances, reaching 5.39 au at aphelion on 3rd October 2012, the solar arrays could not provide sufficient power for normal spacecraft operations. The on-board timer was set to initiate the wake-up of the spacecraft 31 months later at 10:00 UTC on 20th January 2014.

1.2 Rosetta Spacecraft

In normal mode Rosetta is three-axis stabilised. Attitude measurement and control makes use of autonomous star trackers and ring laser gyros with, usually, four reaction wheels running. Deep space communications are via the steerable, two-degree of freedom high-gain antenna (HGA).

The spacecraft carries four cameras: two identical, so-called NAVCAMs, whose primary purpose is for optical navigation; and two cameras of the OSIRIS (**O**ptical, **S**pectroscopic, and **I**nfrared **R**emote **I**maging **S**ystem) science instrument, the Narrow-Angle Camera (NAC) and the Wide-Angle Camera (WAC).

For entry into the hibernation mode, Rosetta was spun-up to a gentle rotation of about one revolution every 90 seconds. The spin-axis direction was chosen so that at aphelion it would point towards the Sun and the fixed rotation angle of the arrays was chosen such that then they would be face-on to the Sun direction. At reactivation, spin-down and spacecraft slewing were performed autonomously so that the arrays were Sun pointing and the HGA Earth-pointing.

2. Reactivation

On 20th January 2014, Rosetta was 4.5 au from the Sun, 5.3 au from the Earth and 9.2 million km from 67P/C-G. For generating the ground antenna pointing predictions, the orbit was propagated starting from the last determination before hibernation. The main source of uncertainty was the acceleration due to solar radiation pressure. As estimated during the earlier cruise phases, a scale factor correction of +6% was presumed with a conservative 1σ uncertainty of 3%. Even so, the 3σ value for the semi-major axis of the error ellipse on the plane-of-sky was equivalent to only 0.2 millidegrees, at least two orders of magnitude smaller than the half-power-beam-width of the deep space antennas: thus there was no concern with the pointing predictions.

Taking into account the duration needed for the spacecraft's autonomous actions, including several hours for warming up the star trackers, plus the one-way light-time, detection of the spacecraft signal was expected at 18:00 UTC. After anxious waiting, 18 minutes later the reception of the S-band signal was confirmed at the two NASA/DSN 70 m antennas at Canberra and Goldstone. Subsequent analysis of the telemetry showed that during hibernation the on-board software had unexpected problems which were cured by re-booting the on-board processor and this ultimately led to the delay. On the same day, the X-band downlink was switched on and six days later the uplink was switched from S-band to X-band.

Using the interplanetary orbit determination system [5, 6], the spacecraft's trajectory was accurately reconstructed after a few days of acquiring two-way Doppler and range data at the ESA 35 m antenna in New Norcia in Australia and at stations in the three NASA/DSN complexes. Later on, Rosetta was also often tracked from the ESA 35 m stations at Cebreros in Spain and Malargüe in Argentina. The default, highest ranging code previously used at ESA stations led to a two-way range ambiguity of 4626 km. The 3σ uncertainty in the spacecraft's geocentric distance at reactivation was 2576 km. Since the ambiguity can be resolved in the orbit determination only if the two-way range is known to better than half the two-way ambiguity, as a temporary precaution the highest code was increased by two, giving a four fold increase in the ambiguity factor. It turned out that the prediction made for Rosetta's position at reactivation was in error by just 500 km.

3. Comet Orbit Determination

3.1 Ground-based Astrometry

After reactivation, Rosetta's velocity relative to the comet was 800 m/s and aligned very close to the target's predicted direction. The comet's predicted trajectory was based on a long-arc orbit solution that used only ground-based astrometric data from 1988 until 5th October 2013. During the following winter the solar elongation was too low for acquiring observations. On the assumption that the maximum comet activity occurred at perihelion, the estimate for the transverse component of the standard non-gravitational force model [7] was positive, indicating that the comet's rotation was prograde (that was later confirmed during the close approach phase).

More astrometric data were acquired, starting on 28th February. Including them in the orbit determination led to a change in the comet's estimated position of 1200 km but with a formal 1σ uncertainty almost as large as the change. This was considered to be an optimistic evaluation mainly because the data had to be reduced using a star catalogue known to suffer from significant zonal biases [8] but also because of limitations in accurately modelling the non-gravitational forces.

3.2 Comet Detection On-board

The two NAVCAMs have a circular field-of-view with a diameter of 5° and can detect objects down to visual magnitude 12. Seen from Rosetta, the comet was not expected to reach this brightness until the first half of May at the earliest. The manoeuvre plan - see section 4 - called for a series of ten individual trajectory control manoeuvres (TCMs) to reduce the spacecraft's velocity relative to 67P/C-G in steps down to less than 1 m/s at arrival at the comet. Although not a requirement, it was considered highly desirable to improve the knowledge of the comet's relative state before the TCMs began. But the first one, a test burn, was scheduled for 7th May and the second, the individually largest TCM, two weeks later.

The OSIRIS NAC is much more sensitive and the OSIRIS team agreed to provide their images for navigation purposes. The NAC field-of-view (FOV) is 2.2° x 2.2°, less than half that of the NAVCAMs, but even with the most pessimistic assumptions on possible errors in the comet's relative direction, it was considered certain that it would appear in the FOV.

On 20th March, when still 4.9 million km from the comet, an object was identified in NAC images 22 millidegrees from the expected location and moving across the sky with the expected speed and direction of the comet.

3.3 Optical Navigation

Starting on 24th March, every three days, three NAC images were acquired. Including the reduced data from the first six images in the orbit determination changed the comet's estimated relative position by 2020 km.

The first NAVCAM images with comet detection were acquired on 8th May at a relative distance of 1.8 million km. Thereafter, up to five images were acquired every day. Up to early July, the comet remained a point-like object and the optical navigation, using reduced data from both cameras, was made in the same way as during the approach phases of the asteroid fly-bys [3, 4]. In the reduction process the background stars in the images were used to determine the direction to the comet and these data augmented the spacecraft radiometric data so that the solar system barycentric states of both objects were determined and, of most importance, the position and velocity of the comet relative to Rosetta. At the end of May, the 3σ uncertainty of the separation distance, then slightly more than 500 000 km, was 400 km.

Figure 1 shows the post-fit optical data residuals up to the end of May. The NAVCAM pixel size is 5 millidegrees. The NAC CCD is 2000 x 2000 pixels so it has a resolution almost five times better than the NAVCAM. The standard deviation of the residuals is about one-tenth of a pixel for both cameras. On some occasions, for example on 7th April, the image processing was adversely affected by a star being very close to the comet so these data were deweighted in the orbit determination.

After 6th June, only the NAVCAM provided images for optical navigation during the close approach phase.

Figure 2 shows the variation in the direction of the comet, as seen from Rosetta, during the first half of May. Also plotted is the path as it was predicted more than three years earlier, before hibernation. The difference between the two is only about one-tenth of a degree.

4. Manoeuvre Plan

As explained in detail in [9], there were two main drivers for the design of the manoeuvre strategy. One was robustness: the need to have a sufficient time margin if, for any reason, a manoeuvre could not be performed at the planned time so that it could still be executed well before flying past the comet. For the first main manoeuvre, the margin was 14 days and then, with decreasing relative velocity, reduced in steps down to 3 days for the final rendezvous manoeuvre. The other driver was to aim continuously not directly at the comet but with an off-set so that its apparent motion against the stellar background would provide information on the separation distance. Initially, this off-set was set to 50000 km and reduced in steps down to 200 km for the penultimate manoeuvre. This meant that the relative trajectory had a very slight spiral appearance. The penalty for the required extra propellant was insignificant.

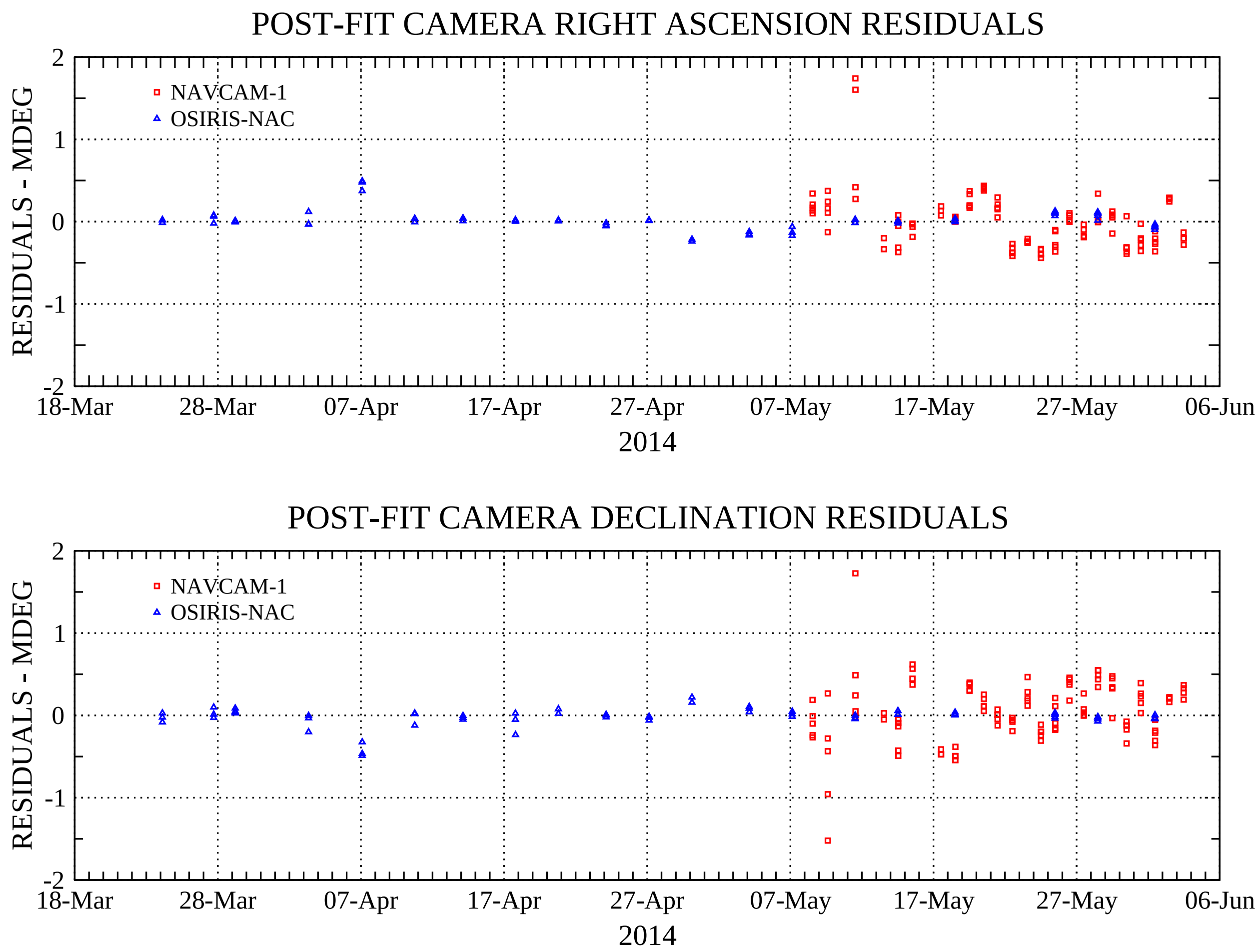

Figure 1. Post-fit optical data residuals

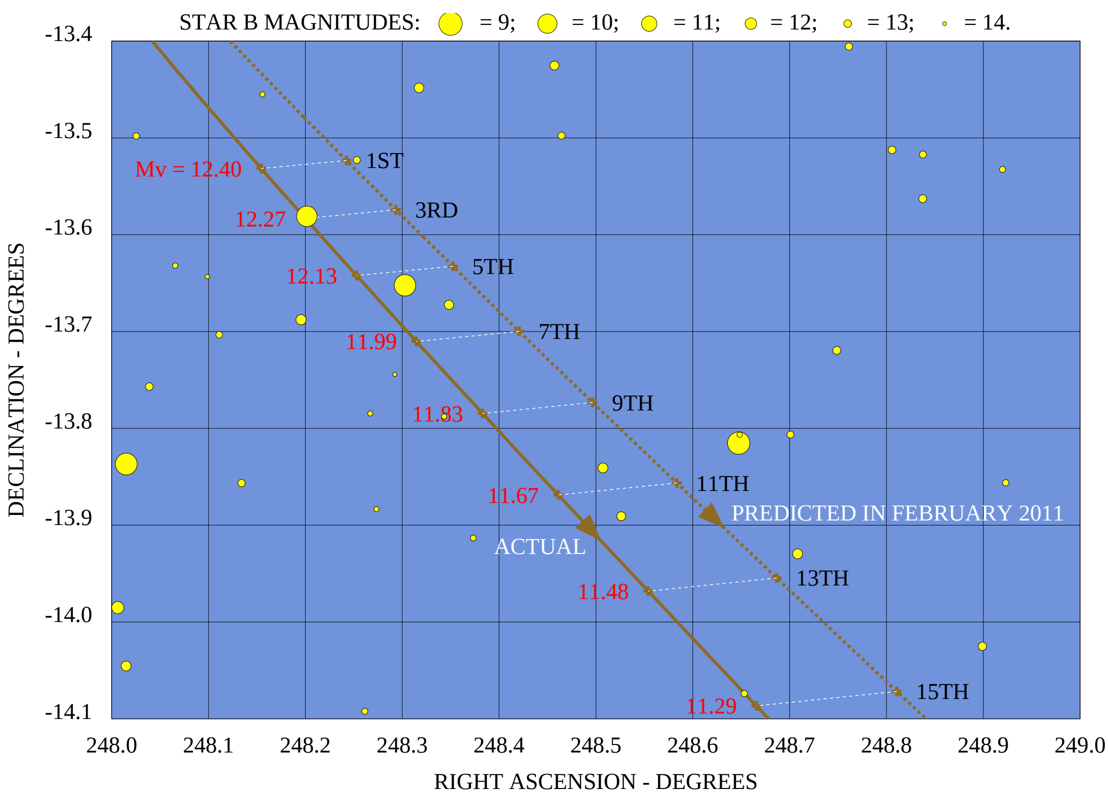

Figure 2. Comet direction from Rosetta in the first half of May 2014

Figure 3 shows the orbits of Rosetta and 67P/C-G (in brown). The braking TCMs were to occur during the arc shown in red. Figures 4, 5 and 6 show the ecliptic projection of the expected motion of Rosetta relative to the comet in May, June and July 2014. In all three plots the comet is at the origin. The scale of Fig. 4 is about 4 times larger than Fig. 3 and the scale of Fig. 5 is about 9 times larger than Fig. 4. The individual TCMs shown are those that were already planned in 2012. The first four TCMs were to be executed during what was called the near comet drift (NCD) phase and the next four in Fig. 6 during the "far approach trajectory" (FAT) phase. The final two smallest TCMs during the "close approach trajectory" (CAT) phase are not shown. The reduction in the relative velocity after each TCM can be appreciated from the shortening of the lengths between the tick marks shown every five days.

5. Delta Differential One-Way Range (ΔDOR)

To achieve the best possible accuracy for the orbit determination and especially calibrations of the TCMs, starting on 28th April the radiometric data were augmented with differential one-way range (DOR) measurements. After correlating such measurements, the resulting ΔDOR data points from two pairs of station baselines, whose orientations are quite different, provides very precise information for the spacecraft's location on the plane-of-sky [10]. ΔDOR data acquired a few days apart substantially improves the knowledge of the spacecraft's velocity component on the plane-of-sky. So four sessions of DOR measurements were scheduled between the times of each TCM. Each session lasted one hour, allowing five scans between the spacecraft and calibrating quasar and hence two ΔDOR data points from the correlation process.

The DOR sessions were scheduled predominantly for the ESA stations on the Cebreros-New Norcia and Cebreros-Malargüe baselines. Four sessions of measurements used two NASA/DSN 34 m antennas on the Goldstone-Canberra baseline and colleagues at JPL correlated these DOR data. In mid June the spacecraft was deep in the southern hemisphere so that there was a long enough interval of mutual visibility from both New Norcia and Malargüe. Two ΔDOR data points were successfully obtained from this baseline on 12th June.

For the first month of ΔDOR data, their fit in the orbit determination process was unsatisfactory and led to a scatter in the residuals substantially higher than had been expected. For several weeks it could not be resolved whether the problem was with the data or the modelling of the spacecraft dynamics. The underlying cause was finally found and corrected for all the ESA DOR data acquired after 20th June.

The Rosetta transponder does not have the capability to generate DOR tones. Instead, the harmonics of the telemetry subcarrier have to be used. The correlator needs to know the subcarrier frequency to high accuracy and this was determined early in the mission. Due to a reboot during hibernation, the clock driving the on-board timing system had switched and ticked at a slightly different rate from that of the clock previously used and so altered the subcarrier frequency by a fraction of 1 Hz.

All of the ΔDOR residuals are plotted in Fig. 7. The improvement in the data quality after the re-estimation of the subcarrier frequency within the correlation process is obvious. The standard deviation of these residuals is well below 0.5 ns. An error of this size for the Cebreros-New Norcia baseline, at a geocentric distance of 2.76 au (as it was on 6th July) corresponds to a position error on the plane-of-sky of less than 6 km.

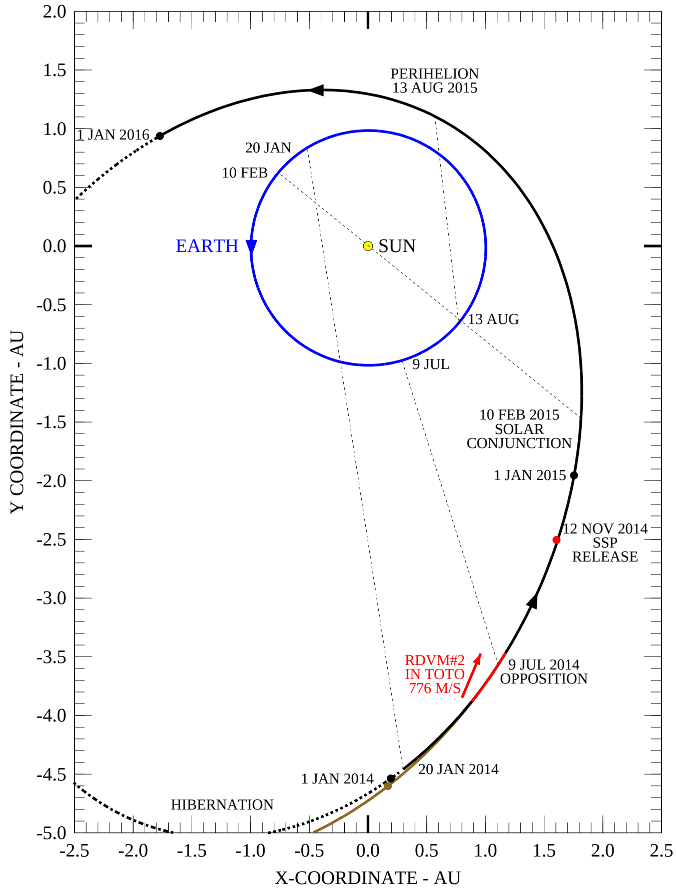

Figure 3. Rosetta Orbit - Ecliptic Projection

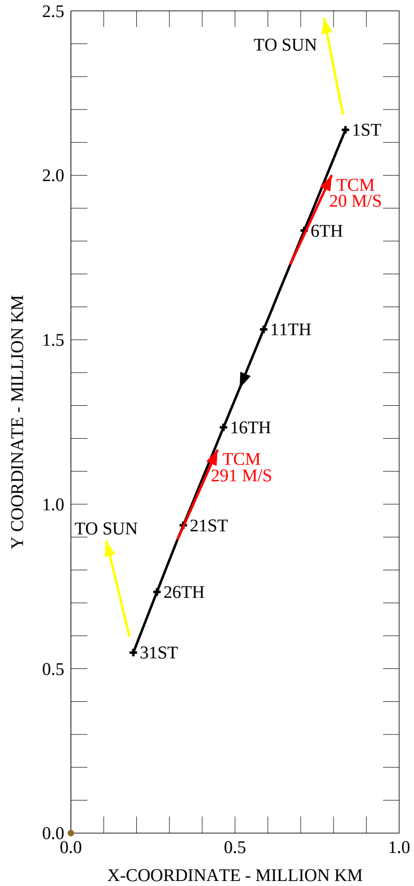

Figure 4. Rosetta relative to comet in May

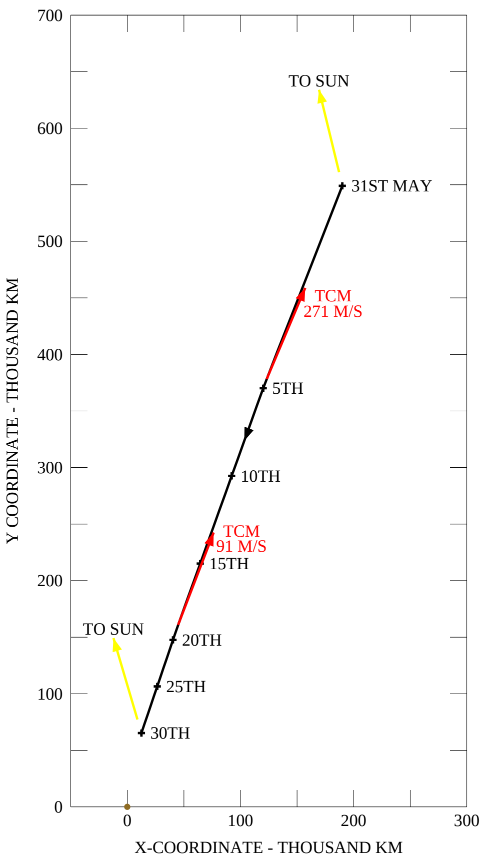

Figure 5. Rosetta relative to comet in June

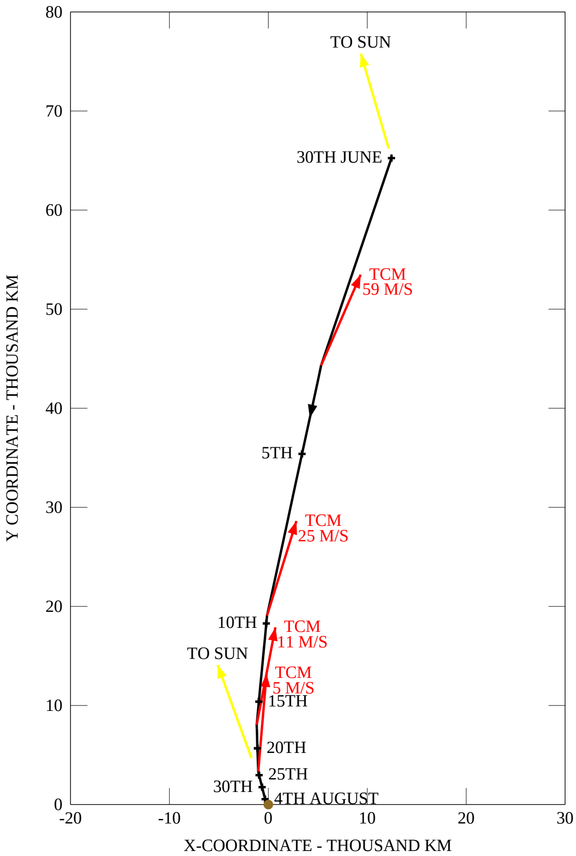

Figure 6. Rosetta relative to comet in July

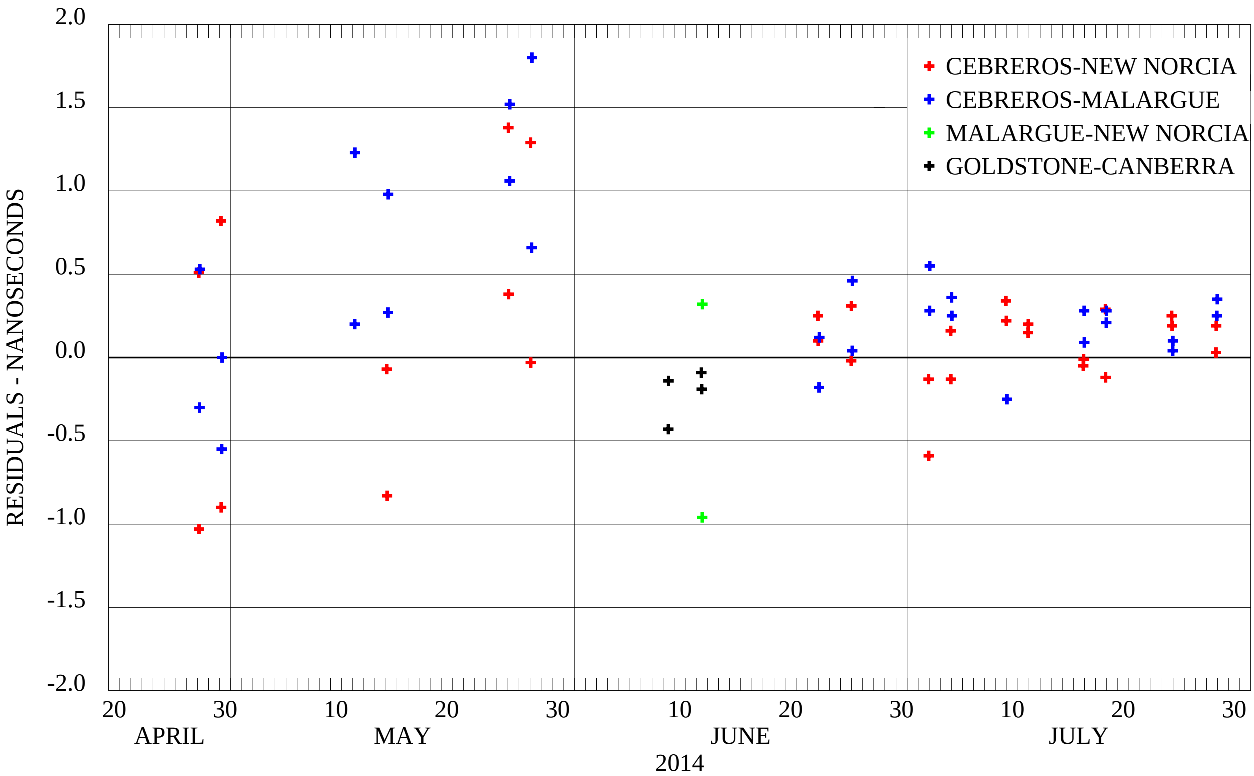

Figure 7. Rosetta post-fit ΔDOR residuals

6. Trajectory Control Manoeuvres

6.1 Manoeuvre Monitoring

Except for the two CAT TCMs, the HGA was kept Earth-pointing throughout each manoeuvre so near real-time monitoring was possible. As soon as files of raw Doppler data, sampled once per second, became available, two so-called pass-throughs of the data using the predicted orbit were made and the residuals plotted. One was without the TCM modelled and the other included the expected acceleration profile throughout the manoeuvre. The resulting variations in the two-way range-rate residuals are illustrated in Fig. 8 for the NCD-2 TCM whose nominal magnitude was 269.485 m/s.

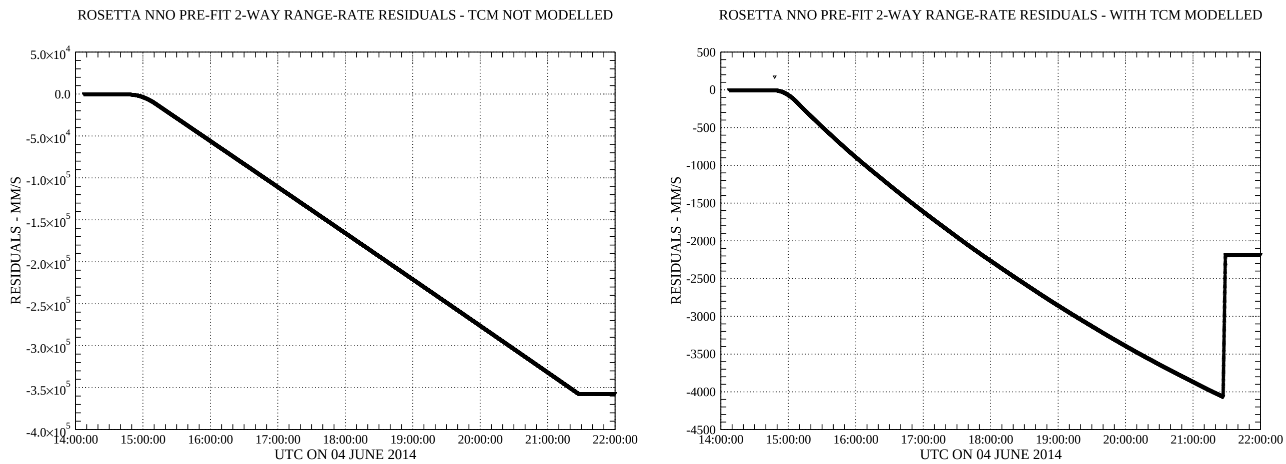

Figure 8. Rosetta pre-fit two-way range-rate residuals

Each Rosetta TCM starts with a liquid settling phase lasting 20 minutes during which the thrust is ramped to its steady state value. This accounts for the curvature on the left plot at the beginning of the manoeuvre execution. Throughout the following six hours the acceleration appeared steady (although the plot scale precludes being able to discern small variations from a straight line). By magnifying the scale, the precise start and stop times of the manoeuvre were determined.

The TCM reduced the spacecraft's range-rate so the negative slope on the right plot shows that the burn performance was continuously higher than predicted. Except for the last TCM, the duration of all the manoeuvres was controlled by accelerometers. For the NCD-2 TCM, the burn was stopped 123 seconds earlier than the predicted end time which accounts for the near vertical line on the plot. Even so, the final residual values of about -2.2 m/s meant that the manoeuvre overperformed.

Before the burn, the spacecraft had been slewed to an attitude such that the ΔV direction should have been 48.892° from the direction to Earth. The expected change in two-way (geocentric) range-rate was -354.363 m/s. If the manoeuvre direction was perfect, the calibration would be an overperformance of 0.62%. The final calibration - see section 6.3 - was made after several days more of radiometric data, including the ΔDOR data. For orbit determination purposes, the raw Doppler data were compressed to 60 seconds count times but the data during manoeuvres were omitted because of the difficulties in modelling precisely the actual profile of the acceleration.

Figure 9 shows the two-way range-rate residuals over a 4 minutes interval starting shortly after the end of the NCD-2 TCM. The oscillatory signal has an amplitude of about 3 mm/s and a period between 13 and 14 seconds. Only many minutes later can the oscillation not be clearly seen above the data noise. This is explained by the first flexible mode of the solar arrays that was expected to have a period of about 16 seconds. Such an oscillation of the HGA phase centre means that the tips of the arrays were oscillating with an amplitude of the order of 15-20 cm. The virtually identical behaviour was seen after the end of all but the smallest TCMs.

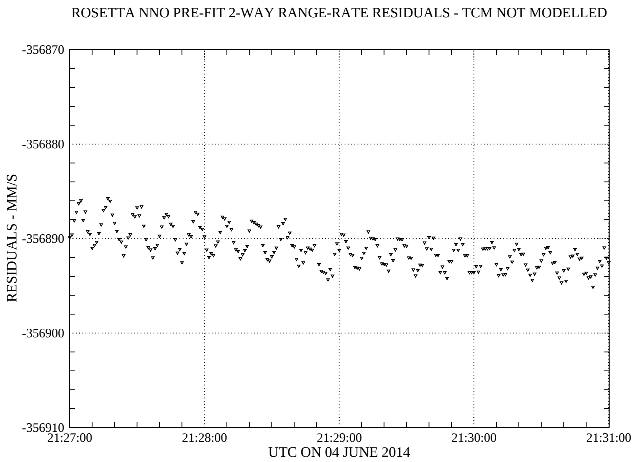

Figure 9. Rosetta post-TCM range-rate residuals

6.2 Outgassing

Before hibernation, almost all the time Rosetta's attitude was maintained such that the solar array (spacecraft Y) axis was perpendicular to the Sun direction and the Sun shone in the quadrant between the +X and +Z spacecraft axes. The -X face, where the Philae lander was mounted, and the -Z face, where the 10 N thrusters are located, were almost always in shadow and very cold.

On occasion, mainly associated with thermal tests, the spacecraft was slewed so that the Sun shone obliquely on the -Z face. After most of these events, good fits to the Doppler data could not be achieved without allowing the estimation of an "autonomous" manoeuvre. This was attributed to outgassing: fluid, mainly water, within the spacecraft, migrating to the external surfaces, freezing and accumulating on the cold face and them being sublimated when illuminated by the Sun. The estimated ΔV component in the +Z direction was sometimes more than 1 mm/s.

Similar features were observed during the comet approach phase. The boresights of the cameras and other scientific instruments are aligned along +Z axis and for most of the time this axis was pointed towards the comet. As can be seen in Figs. 3-5, this meant that the Sun shone obliquely on the -Z face and also on the +X face so that the base plate of the lander remained in shadow. On 19th May and 26th June the spacecraft attitude was changed so that the Sun shone directly on the -Z face for 75 minutes. Unexpected deviations in reaction wheel speeds and in the Doppler data, presumably due to outgassing, were again observed. Sublimation of ice on the lander base plate could explain the torque. Its estimated value was lower on the second occasion but on both occasions the estimated ΔV along +Z was about 0.5 mm/s.

Related phenomena also occurred after the initial manoeuvres. For TCMs the thrust direction is along +Z, so as can also be seen in Figs. 3-5, for executing them Rosetta had to be slewed through almost 180°. After the slew back to comet-pointing following the large NCD-1 and NCD-2 TCMs, a satisfactory fit of the Doppler data could again not be achieved without allowing for a small velocity change.

In order to understand better what was happening, for the NCD-3 TCM, the ROSINA instrument was switched on. The experiment makes pressure measurements and analyses the gas environment around the spacecraft. The Principal Investigator reported [11] concentrations of both water and hydrazine during the return slew. The first steep rise of the pressure data occurred very shortly after it began. A second sharp rise occurred at the time the -Z face started to become illuminated by the Sun. Following both rises, the subsequent profiles were approximately exponential decays. Even after more than a day, the pressure measurements were still higher than before the slew.

In the orbit determination, the best fit to the Doppler data was achieved by estimating a 2.3 mm/s impulsive ΔV shortly after the slew followed by a total integrated acceleration over the following two days of about 0.9 mm/s. It was concluded that the cause was products of combustion initially adhering mainly to the -Z face of the spacecraft but providing reactive forces on leaving the spacecraft surfaces when exposed to sunlight.

As the size of the succeeding TCMs became progressively smaller, so did the ΔV perturbations due to outgassing. After the two CAT manoeuvres nothing spurious was observed.

6.3 Manoeuvre Performances

All the TCMs were successfully executed at the foreseen times. The final calibration details are listed in Tab. 1. Except for the pre-set magnitude of the NCD test TCM, before each manoeuvre the whole of the rest of the sequence up to arrival at the comet was re-optimised. A comparison of the finally planned individual NCD and FAT TCMs with those depicted in Figs. 4-6 shows that they were all very little different from the nominal plan drawn up during Rosetta's hibernation.

Table 1. Trajectory Control Manoeuvres

Date in 2014	Name	Duration		ΔV		
		Planned H:MM:SS	Actual M:SS	Planned m/s	Calibrated m/s	Calibrated %
07 May	NCD test	40:20	-0:36	20.000	+0.013	+0.07
21 May	NCD-1	7:18:42	-2:08	289.590	+1.332	+0.46
04 June	NCD-2	6:41:02	-2:03	269.485	+1.509	+0.56
18 June	NCD-3	2:16:41	-0:39	88.733	+0.524	+0.59
02 July	FAT-1	1:33:13	-1:04	58.701	+0.027	+0.05
09 July	FAT-2	46:32	-0:30	25.718	-0.005	-0.02
16 July	FAT-3	25:51	-0:20	10.963	-0.015	-0.13
23 July	FAT-4	16:34	-0:11	4.823	+0.008	+0.17
03 August	CAT pre-insert	13:12	-0:05	3.206	-0.070	-2.17
06 August	CAT insertion	06:26	*	0.892	+0.019	+0.21

* Not recorded.

Due to the excellent performance of the accelerometers, all of the estimated ΔV magnitudes were within 1% of the planned values except for the CAT pre-insertion manoeuvre. The formal calibration uncertainties were tiny but have not been listed because they are unrealistically small due to the difficulties in modelling the dynamical events shortly after each post-manoeuvre slew. However, their real uncertainties are still likely to be only a tiny fraction of a percent.

The exception mentioned above was thought very likely to be due to accelerometer bias miscalibration. The performance of the accelerometers is sensitive to their temperatures which, in turn, depend upon the spacecraft attitude. Therefore, when possible, the accelerometer bias calibration was made when in the TCM attitude. For the CAT pre-insertion manoeuvre this was not possible. Also, there was very little time between the end of the slew to the manoeuvre attitude and its execution, hence little time for accelerometer stabilisation. As a consequence, the final CAT manoeuvre duration was controlled by the impulse count method.

7. Final Approach

In early July the comet began appearing as an extended object in the NAVCAM images. As it grew in size, the scatter in the optical data residuals increased and some trends developed due to limitations in identifying the true centre of the comet when observing at a slowly varying solar phase angle above 30°. For example, on 31st July, when the image shown as Fig. 10 was acquired, and at 1284 km distance, 5 km (roughly the longest axis of the comet) was equivalent to an angular size of 0.223° or almost 45 pixels of the NAVCAM. The scatter in the optical right ascension residuals was then up to 4 pixels and in the declination residuals up to 2 pixels.

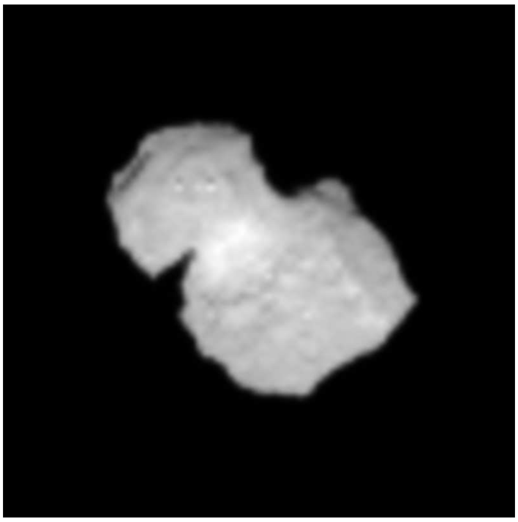

Figure 10. 67P/C-G on 31st July 2014

This modelling problem had no influence on the safe arrival of the spacecraft at the comet. The second CAT manoeuvre on 6th August inserted the spacecraft into a hyperbolic trajectory around the comet with a pericentre distance of 80 km and an initial solar phase angle of 50°. The spacecraft was then 3.6 au from the Sun and 2.7 au from the Earth. Since about four days earlier, the gravitational attraction of 67P/C-G had become the primary force acting on the spacecraft and already a good preliminary estimate had been obtained for the comet's GM value and hence mass. Then began the most challenging and demanding navigation activities, which included the precise characterisation of all of the comet's kinematic parameters.

8. Conclusions

After its reactivation, the Rosetta navigation activities during the approach phase to 67P/C-G followed very closely what had been planned and tested, mostly during the preceding 31 months while the spacecraft was in hibernation. Once the comet had been detected on-board, the optical data acquisition and image processing, combined with the decreasing separation distance, meant that continuously better estimates were obtained of the comet's position and velocity relative to Rosetta.

There were just two unexpected but relatively minor problems related to navigation. One was the somewhat degraded quality of ΔDOR data whose cause was found and corrected (and a lesson learned). The other was explained with the help of the ROSINA science instrument: outgassing during and after slews following large manoeuvres was shown to be the reason for apparently anomalous Doppler data and deviations in reaction wheel speeds.

Rosetta arrived at 67P/C-G after a ten years cruise around the solar system. The primary function of the mission - in situ scientific observations of a comet - then began. Due to the excellent performance of the large manoeuvres (including those before hibernation), there remained sufficient propellant to make these observations over a prolonged period and over a large range of heliocentric distance and hence of comet activity level.

9. References

[1] Morley, T. and Budnik, F., "Rosetta Navigation at its First Earth Swing-by", Proceedings 19th International Symposium on Space Flight Dynamics - 19th ISSFD, Kanazawa, Japan, 2006.

[2] Budnik, F. and Morley, T., "Rosetta Navigation at its Mars Swing-by", Proceedings 20th International Symposium on Space Flight Dynamics - 20th ISSFD, Annapolis, MD, USA, 2007.

[3] Morley, T. and Budnik, F., "Rosetta Navigation for the Fly-by of Asteroid 2867 Šteins", Proceedings 21st International Symposium on Space Flight Dynamics - 21st ISSFD, Toulouse, France, 2009.

[4] Morley, T., Budnik, F. Croon, M. and Godard, B., "Rosetta Navigation for the Fly-by of Asteroid (21) Lutetia", Proceedings 23rd International Symposium on Space Flight Dynamics - 23rd ISSFD, Pasadena, California, USA, 2012.

[5] Budnik, F., Morley, T. and Mackenzie, R., "ESOC's System for Interplanetary Orbit Determination", Proceedings 18th International Symposium on Space Flight Dynamics - 18th ISSFD, Munich, Germany, 2004.

[6] Muñoz, P. *et al*., "Preparations and Strategy for Navigation during Rosetta Comet Phase", Proceedings 23rd International Symposium on Space Flight Dynamics - 23rd ISSFD, Pasadena, California, USA, 2012.

[7] Marsden, B., Sekanina, Z. and Yeomans, D., "Comets and nongravitational forces. V.", The Astronomical Journal, Vol. 78, No. 2, March 1973.

[8] Chesley, S., Baer, J. and Monet, D., "Treatment of Star Catalog Biases in Asteroid Astrometric Observations", Icarus 210, 158-181, 2010.

[9] Herfort, U. and Casas, C., "Trajectory Preparation for the Approach of Spacecraft Rosetta to Comet 67P/Churyumov-Gerasimenko", Proceedings 25th International Symposium on Space Flight Dynamics - 25th ISSFD, Munich, Germany, 2015.

[10] Maddè, R. *et al*., "Delta-DOR - A New Technique for ESA's Deep Space Navigation", ESA Bulletin, No. 128, 68-74, November 2006.

[11] Altwegg, K., "Report on Sniff Test - 18/20 June 14", Rosetta ROSINA RO-ROS-TR-1163, Issue 1.1, June 2014.